Integrated Optimisation of Transit Networks with Schedule- and Frequency-Based Services Subject to the Bounded Stochastic User Equilibrium

Yu Jiang[a], Thomas Kjær Rasmussen[a], Otto Anker Nielsen[a]

[a] Transport Modelling Division, Department of Management, Technical University of Denmark

Corresponding author: yujiang@dtu.dk

ABSTRACT

In many European metropolitan areas, the urban transit system is a mixture of schedule- and frequency-based services. This study proposes an integrated transit frequency and schedule design problem (ITFSDP), where frequencies and schedules are simultaneously determined, and develops a bi-objective model for the ITFSDP to minimise operation costs and total passenger-perceived generalised travel cost. Meanwhile, the passengers' route choice behaviour is described by the bounded stochastic user equilibrium (BSUE). The in-vehicle congestion effect is represented using a set of constraints that differ in terms of the sitting and standing costs as sitting and standing passengers perceive crowding differently. This set of constraints captures the realistic behavioural feature that having occupied a seat, users remain seated at subsequent stops in the same vehicle. The problem is formulated as a mixed integer nonlinear programming problem, which is subsequently linearised to a mixed integer linear programming problem and solved using a branch-and-bound algorithm. A column generation-and-reduction phase is embedded in the solution algorithm to obtain the bounded choice set according to the BSUE constraints. Experiments are conducted to illustrate the model's properties and the performance of the solution method. In particular, we demonstrate a Braess-like paradoxical phenomenon in the context of transit scheduling and highlight that well-synchronised transit services can deteriorate the network performance in terms of the total passengers' generalised travel cost when considering passenger congestion costs due to crowding.

Keywords: Public transport; Transit frequency and schedule design; Stochastic user equilibrium; Bounded choice model; Bilevel programming

1. INTRODUCTION

The existing studies on public transport planning address the transit frequency setting and the timetabling problems separately and do not simultaneously focus on both problems (Ceder and Wilson 1986; Guihaire and Hao 2008). However, many European urban transit systems involve a mixture of systems, such as frequency-based services in the centre and schedule-based services in the suburbs, and many passengers rely on more than one type of service to complete a journey. For example, in Greater Copenhagen, bus line 150S is operated based on frequency; specifically, the number of runs per hour departing from the terminal is predetermined by the operator (Movia 2020a). In contrast, bus line 350S is operated based on a schedule; specifically, a predetermined timetable is provided to passengers, and the operator must comply with the timetable (Movia 2020b). Meanwhile, passengers travelling between Lundtofteparken and Elmegade may need to transfer from 150S to 350S (see Appendix A for an overview from Google Maps). To enhance the coordination for providing a seamless travel experience to retain existing users and attract new users, it is of practical significance to simultaneously design the two types of services. In this study, this problem is named as integrated transit frequency and schedule design problem (ITFSDP) and a bi-objective optimisation model is developed to solve it. To be more specific, the frequencies associated with frequency-based lines and the timetables related to the schedule-based lines are determined to minimise operation costs and total passenger-perceived generalised travel cost. In addition to considering operational constraints associated with the two types of services, we also incorporate constraints to characterise passengers' route choice behaviour and capture a realistic seating behaviour such that once having occupied a seat, users remain seated at subsequent stops in the same vehicle. To a certain extent, the considered problem can be viewed as that of determining the frequency and schedule for high- and low-frequency lines, respectively. However, we label the services of high- and low-frequency lines as frequency- and schedule-based services, respectively, as our considered problem is more general in the sense that lines operating based on a schedule or frequency do not necessarily have a low or high frequency, respectively. This situation is in accordance with the existing public transport system in Copenhagen (Eltved et al. 2019; Gardner et al. 2021).

1.1. Literature Review

Transit network design problems have received considerable attention over the last two decades. Such problems involve five stages, namely, network design, frequency design, schedule design, vehicle scheduling, and crew scheduling (Ceder and Wilson 1986). A comprehensive discussion of all stages of the transit network design problem has been provided by Guihaire and Hao (2008), Schöbel (2017), Farahani et al. (2013), Cancela et al. (2015) and Ibarra-Rojas et al. (2015). Since this study aims at determining frequencies and schedules, we focus on reviewing the literature related to the frequency design and schedule design stages.

To solve the frequency design problem, Borndörfer et al. (2007) developed a multicommodity flow model in which passengers can be freely routed to minimise the total travel cost. Bertsimas et al. (2021) extended this model by considering the passengers' transfer behaviour. Goerigk and Schmidt (2017) developed a bilevel mixed integer programming model to determine the frequency, assuming that the passengers select the shortest path in the lower level. Szeto and Jiang (2014) incorporated hard capacity constraints into the lower-level transit assignment model and developed a metaheuristic algorithm based on the Karush–Kuhn–Tucker conditions of the lower-level problem to derive the descent direction for updating frequencies. Martínez et al. (2014) formulated a mixed integer linear programming (MILP) model that avoided the bilevel structure and proposed a metaheuristic algorithm for solving large network applications.

To solve the schedule design problem, several researchers have focused on the schedule-synchronisation problem via a mixed integer programming approach. Ceder et al. (2001) and Ceder and Tal (2001) considered the number of simultaneous bus arrivals and proposed a mixed integer formulation to determine the departure times of buses. Ibarra-Rojas and Rios-Solis (2012), Ibarra-Rojas et al. (2016) and Fouilhoux et al. (2016) explicitly devised a binary decision variable representing the feasibility of synchronisation and determined a schedule to maximise the number of synchronisations. Instead of counting the number of synchronisations, Wong et al. (2008) directly minimised the passengers' waiting time, which was expressed as a set of constraints. Ávila-Torres et al. (2018) developed a model to determine the frequency and schedule in an integrated manner. However, in their model, the frequency was computed in a pre-processing step instead of being simultaneously optimised with a schedule.

The existing approaches aim at optimising the services of a fleet operated homogeneously, i.e., based on either frequency or schedule. In practice, transit lines or fleets owned by different operators may operate differently. In this scenario, commuters may rely on more than one type of service to complete a journey (Eltved et al. 2019). In this context, it is desirable to develop an integrated optimisation model, similar to a multimodal transport network design problem, which may be more effective than the existing approaches when different transport modes are jointly considered (Bertsimas et al. 2020).

To consider the passengers' route choice behaviour in a frequency or schedule design problem, the prevailing behavioural assumptions pertain to the user-optimal (Mesa et al. 2014; Schmidt and Schöbel 2015; Szeto and Jiang 2014; Goerigk and Schmidt 2017) and stochastic user equilibrium (SUE) (Li et al. 2010). The SUE is more general than the user-optimal. Notably, a multinomial logit (MNL) SUE model can approximate a user-optimal model by setting a large scaling parameter. Nevertheless, the SUE model is built upon the assumption that each route has a positive probability of being chosen, irrespective of the degree of its nonoptimality. This assumption may not hold in practice due to passengers' time constraints. To address this aspect, Watling et al. (2018) developed a more realistic bounded SUE (BSUE), assuming that passengers only consider alternatives with costs within a cost bound to the minimum cost alternative. The BSUE model is more general than the MNL SUE model as the MNL SUE model has been proven to be a special case of the BSUE model when the bound approaches infinity. Therefore, in this study, the BSUE is used to reflect the passenger route choice behaviour.

In existing studies on frequency and schedule design, the effect of sitting and standing in modelling the in-vehicle congestion has not been considered. Intuitively, the aspect of a passenger being seated influences the comfort level, which affects the passengers' route choice. This aspect has been empirically demonstrated in several studies (Wardman and Whelan 2011; Tirachini et al. 2016; 2017), which indicated that standing and sitting are valued differently by passengers. Although the effects of seating have been modelled in transit assignment models (Hamdouch et al. 2011; Schmöcker et al. 2011; Leurent 2014; Cats et al. 2016; Tang et al. 2020), they have not been incorporated into a model to determine either frequencies or schedules.

1.2. Paper contributions and structure

The main contributions of this study are as follows. Firstly, we propose a new ITFSDP. Practically, it applies to an urban transit system where transit lines are operated in a mixed manner, i.e., some are based on the frequency, and some are based on the schedule. It differs from existing studies that determine the services of a fleet operated with only one type of service. Secondly, we develop a bi-objective optimisation model for the ITFSDP to minimise operation costs and total passenger-perceived generalised travel cost. It considers passengers' route choice behaviour described by the BSUE. Furthermore, it uses a set of constraints to capture a realistic seating behaviour such that once having occupied a seat, users remain seated at subsequent stops.

The remainder of the paper is structured as follows. Section 2 introduces the assumptions and notations used in this paper and describes the formulation of the ITFSDP. Section 3 introduces the solution algorithm. Details of the numerical studies are presented in Section 4. Finally, Section 5 summarises our findings.

2. MATHEMATICAL FORMULATION

2.1. Problem Statement

We consider a finite planning horizon $[0,T]$ for a transit network that contains both frequency- and schedule-based lines. The sets of links, nodes and lines in the network are denoted by E, N, and L, respectively. Each link $e \in E$ in the network is defined by a 3-tuple, $e = (i, j, l)$, which contains three elements, namely, tail node $i \in N$, head node $j \in N$, and transit line $l \in L$. Correspondingly, we use $t(e)$, $h(e)$, and $\ell(e)$ to map the tail node, head node, and transit line associated with link $e \in E$, respectively. The in-vehicle travel time associated with link $e \in E$ is given by T_e.

The sets of frequency- and schedule-based lines are respectively denoted as L_{fre} and L_{sch} with $L_{\text{fre}} \cup L_{\text{sch}} = L$ and $L_{\text{fre}} \cap L_{\text{sch}} = \varnothing$. A transit line $l \in L$ contains M_l stops, and the sets of stops and links that the line traverses are denoted by $S_l = \left\{ s_l^1, s_l^2, ..., s_l^{M_l} \right\}$ and $A_l = \left\{ e_l^1, e_l^2 ..., e_l^{M_l - 1} \right\}$. A bus of line $l \in L$ has a limited number of seats, denoted as Cap_l^{seat}. For a schedule-based line $l \in L_{\text{sch}}$, the number of runs to be scheduled is Q_l. The maximum and minimum headways are defined as $H_l^{\max}$ and $H_l^{\min}$. In general, to determine the maximum and minimum headways, various factors, such as resource constraints, safety considerations, and demand distribution, must be considered (Chen et al. 2019; Zhang et al. 2020). To the best of our knowledge, most existing studies on the network design problem treat these two values as exogenously defined parameters (for example, Wong et al. 2008; Ibarra-Rojas et al. 2016; Guo et al. 2017). Moreover, several studies do not consider these entities as critical constraints in the model, restrict the frequency (inverse of the headway) to be nonnegative (Borndörfer et al. 2007; Bertsimas et al. 2021), or confine the lower bound of the frequency (upper-bound headway) (Constantin and Florian 1995).

On the demand side, we are given the number of passengers travelling between certain pairs of nodes, known as origin-destination (OD) pairs. The set of all OD pairs is denoted by W. Note that an origin or destination must be a node in the network, but not vice versa. Each OD pair $w \in W$ is defined by four attributes, $w = \left(o^w, d^w, G^w, TD^w \right)$, where $o^w \in N$ and $d^w \in N$ denote the origin and destination nodes, respectively, and G^w represents the number of passengers whose departure time interval is TD^w. As the time horizon is discretised into time intervals, demand G^w consists of all passengers departing within interval TD^w. For simplicity, a passenger's departure time equals the user's arrival time at the first departure transit stop. Passengers travelling between the same origin and destination nodes with different departure time values are treated as different OD pairs owing to their difference in TD^w.

The set of passenger paths connecting OD pair $w \in W$ is denoted by R^w. A passenger path $r \in R^w$ is composed of either one transit line or multiple lines when transfers are involved. To represent this phenomenon, $N_r^{w,\text{transfer}}$ denotes the set of stops at which passengers transfer. The sets of boarding and alighting stops in path $r \in R^w$ are $N_r^{w,\text{transfer}} \cup \left\{ o^w \right\}$ and $N_r^{w,\text{transfer}} \cup \left\{ d^w \right\}$, respectively. At a boarding (alighting) stop $i \in N_r^{w,\text{transfer}} \cup \left\{o^w\right\}$ ($i \in N_r^{w,\text{transfer}} \cup \left\{d^w\right\}$) along path $r \in R^w$, the link that passengers board (alight) is indexed by $e_{r,i}^{w,\text{board}}$ ($e_{r,i}^{w,\text{alight}}$). Correspondingly, the boarding (alighting) line is $\ell\left(e_{r,i}^{w,\text{board}}\right)$ ($\ell\left(e_{r,i}^{w,\text{alight}}\right)$). Finally, we use N_r^w and E_r^w to denote the sets of all stops and links traversed by path $r \in R^w$.

The following assumptions are made throughout the analysis: A1) Travel demand G^w and departure time TD^w are known and deterministic (Nuzzolo et al. 2001; Hamdouch et al. 2011). Although the acquisition of OD data is beyond the scope of this study, it is acknowledged that given the penetration of smart card data and advanced methodologies for OD estimation (Hussain et al. 2021), more detailed OD matrices may be available in the future. In addition, an increasing number of recent studies have assumed that the time-dependent passengers' demand data are known (Shafiei et al. 2020; Yin et al. 2021; Lee et al. 2022). A2) A passenger boards the first arriving vehicle of the transit services on the chosen path. This is commonly used to simplify the computation of the waiting time in research on the transit assignment problem (De Cea and Fernández 1993; Toledo et al. 2010; Cortés et al. 2013). A3) The passengers' travel behaviour is described by the BSUE (Watling et al. 2018). The choice set of used paths is determined by a parameter η that defines a bound on the generalised costs of paths that are considered attractive. Any paths that deviate more than η units from the actual minimum generalised cost path are not considered relevant and assigned a zero choice probability. Paths with costs below the bound defined by η are assigned a positive choice probability.

Based on these assumptions, a bi-objective optimisation model is developed to determine the following key decision variables simultaneously.

1) f_l: Frequency of line $l \in L_{\text{fre}}$ operated based on frequency. The headway associated with line $l \in L_{\text{fre}}$, h_l, is $h_l = {1}/{f_l}$.

2) $\tau_{l,i,q}^{\text{arr}}$, $\tau_{l,i,q}^{\text{dwell}}$, and $\tau_{l,i,q}^{\text{dep}}$: Arrival, dwell, and departure time of the q^{th} run of schedule-based transit line $l \in L_{\text{sch}}$, at stop $i \in S_l$. The dwell time is determined based on the number of boarding and alighting

passengers. Moreover, a minimum dwell time is imposed to reflect that vehicles halt at each stop for a certain duration, and stops cannot be skipped.

3) π_r^w : Generalised travel cost associated with path $r \in R^w$ connecting OD pair $w \in W$. This term is defined as a weighted sum of different path characteristics, including in-vehicle travel time, waiting time, and congestion due to limited capacity. The coefficients associated with each characteristic, β^{inveh}, β^{wait}, and β^{cap}, can be interpreted as users' perceived values for each characteristic and can be calibrated from survey data (Dell'Olio et al. 2011; Anderson et al. 2017; Nielsen et al. 2021). Alternatively, the cost term is similar to the concept of utility, which is a more commonly used term in the literature on using discrete choice models to depict travellers' route choice behaviour. Given E_r^w, which is the set of links traversed for path $r \in R^w$ connecting OD pair $w \in W$, the path in-vehicle travel time can be computed in a straightforward manner. The waiting time can be expressed by a set of constraints (Section 2.3.1). To model the congestion cost associated with capacity constraints, the soft capacity constraint approach is used in this study. In other words, passengers are allowed to board a congested vehicle and thereby induce additional discomfort levels. This phenomenon is consistent with the transit system in Copenhagen and other cities, such as Hong Kong and Beijing. Specifically, we devise a linear function, as described in Section 2.3.2, which includes four parameters: a constant discomfort value independent of the number of passengers (α_0), a coefficient associated with the number of onboard passengers (α_1), a coefficient associated with the number of standing passengers (α_2), and an additional penalty (α_3) that is activated when the vehicle is congested or the number of passengers is more than the number of seats. These parameters can be calibrated with reference to the existing studies on crowding valuation (Wardman and Whelan 2011; Tirachini et al. 2016; 2017).

4) R_{BSUE}^w : Bounded path choice set for OD pair $w \in W$. Multiple paths may exist between an OD pair. According to assumption A3), if path $r \in R^w$ is being traversed by passengers, its generalised travel cost π_r^w must be no higher than a predefined bound value plus the minimum generalised cost of all paths

connecting OD pair $w \in W$. The set of paths satisfying this condition is named the bounded path choice set. In the optimisation model (Section 2.2), the path set is considered as a parameter. However, because the composition of a path depends on frequencies and schedules, the path set cannot be specified in advance. Thus, in the proposed algorithm described in Section 3.1, the path set is iteratively updated through a column generation-and-reduction step.

5) p_r^w : Probability of passengers travelling between OD pair $w \in W$ selecting path $r \in R^w$. The probability of selecting one path from the set is determined by the discrete choice model developed by Watling et al. (2018), which is formulated as constraints in Section 2.2. As the demand associated with an OD pair is known, the number of passengers travelling via a path can be calculated as $G^w p_r^w$.

Table 1 Notation

(a) Parameters

Notation	Description
Network parameters	
T	Time horizon
E	Set of links in the network
N	Set of stops in the network
T_e	Travel time associated with link $e \in E$
$t(e), h(e), \ell(e)$	Tail node, head node, and transit line associated with link $e \in E$
OD-related parameters	
W	Set of OD pairs
o^w, d^w	Origin and destination node of OD pair $w \in W$
TD^w	Departure time associated with OD pair $w \in W$
G^w	Travel demand between OD pair $w \in W$
Route choice model–related parameters	
R^w	Set of paths connecting OD pair $w \in W$
η	Nonnegative bound value to determine the bounded path choice set
R^w_{BSUE}	Bounded path choice set. Set of paths satisfying the condition that the generalised travel cost of any path in the set is no higher than a predefined bound value (η) plus the generalised travel cost of the shortest path connecting OD pair $w \in W$. (Note: This term is considered an exogenous parameter to the nonlinear model described in Section 2.2, whereas it is determined iteratively in the algorithm).
θ	Scale parameter used in the BSUE model
N_r^w	Set of nodes traversed by path $r \in R^w$ connecting OD pair $w \in W$

$e_{r,i}^{w,\text{board}}$, $e_{r,i}^{w,\text{alight}}$	Link in which passengers board or alight at node $i \in N_r^w$ along path $r \in R^w$ connecting OD pair $w \in W$
E_r^w	Set of links traversed by path $r \in R^w$ connecting OD pair $w \in W$
$N_r^{w,\text{transfer}}$	Set of transfer nodes along path $r \in R^w$ connecting OD pair $w \in W$. The sets of boarding and alighting nodes are defined as $N_r^{w,\text{transfer}} \cup \{o^w\}$ and $N_r^{w,\text{transfer}} \cup \{d^w\}$, respectively.
β^{inveh}, β^{wait}, β^{cap}	Coefficients associated with different travel time components, i.e., in-vehicle time, waiting time, and congestion time, for computing the generalised travel cost
$\alpha_0, \alpha_1, \alpha_2, \alpha_3$	Coefficients used to compute the perceived congestion level
α_4	Parameter to represent the number of passengers in terms of the boarding/alighting time. Intuitively, this term represents the average time for a passenger to board/alight a bus.

Transit system parameters

L	Set of all transit lines
L_{fre}, L_{sch}	Set of lines operated based on the frequency and schedule
C_l^{op}	Frequency-dependent operation cost for line l
Cap_l^{seat}	Seating capacity of a vehicle of line $l \in L$
M_l	Number of stops traversed by line $l \in L$
S_l	Set of stops traversed by line $l \in L$, $S_l = \{s_l^1, s_l^2, ..., s_l^{M_l}\}$
A_l	Set of links traversed by line $l \in L$, $A_l = \{e_l^1, e_l^2 ..., e_l^{M_l - 1}\}$
$H_l^{\max}$, $H_l^{\min}$	Maximum and minimum headway of line $l \in L$
$D_{l,i}^{\min}$	Minimum dwell time of line $l \in L$ at stop $i \in S_l$
Q_l	Number of runs to be scheduled for line $l \in L_{\text{sch}}$
α^{weight}	Weighting parameter associated with the operation cost in the objective function

(b) Variables

Transit system-related variables

h_l, f_l	Headway and frequency of line $l \in L_{\text{fre}}$
$\tau_{l,i}^{\text{dwell}}$	Dwell time of line $l \in L$ at stop $i \in S_l$
$\tau_{l,i,q}^{\text{arr}}$, $\tau_{l,i,q}^{\text{dwell}}$, $\tau_{l,i,q}^{\text{dwell}}$	Arrival, dwell, and departure time values of the q^{th} run of line $l \in L_{\text{sch}}$ at stop $i \in S_l$

Route choice-related variables

p_r^w	Probability of selecting path $r \in R^w$ for passengers travelling between OD pair $w \in W$
π_r^w	Generalised travel cost associated with path $r \in R^w$ connecting OD pair $w \in W$
$t_{r,i}^{w,\text{arr}}$, $t_{r,i}^{w,\text{wait}}$, $t_{r,i}^{w,\text{dep}}$	Arrival, waiting, and departure time at stop $i \in N_r^w$ for passengers travelling between OD pair $w \in W$ via path $r \in R^w$
$t_e^{\text{cap,seat}}$	Perceived congestion level for sitting passengers traversing via link $e \in E$
$t_e^{\text{cap,stand}}$	Perceived congestion level for standing passengers traversing via link $e \in E$
$t_{r,e}^{w,\text{cap}}$	Perceived congestion level for passengers of OD pair $w \in W$ traversing link $e \in E$ on path $r \in R^w$

$\Delta_{r,l,i,q}^{w,\text{board}}$	= 1, if passengers travelling between OD pair $w \in W$ via path $r \in R^w$ board the q^{th} run of line $l \in L_{\text{sch}}$; = 0 otherwise
$\Delta_e^{\text{congest}}$	= 1 if the number of passengers onboard is less than the seating capacity when passing through link $e \in E$; = 0 otherwise
$\Delta_{r,e}^{w,\text{seat}}$	= 1 if a passenger of OD pair $w \in W$ using path $r \in R^w$ is seated when traversing link $e \in E$; = 0 otherwise
$v_{l,s_l^k}^{\text{alight}}$	Number of passengers alighting at the k^{th} stop of line $l \in L$
$v_{l,s_l^k}^{\text{board}}$	Number of passengers boarding the k^{th} stop of line $l \in L$
v_e^{onboard}	Number of passengers aboard and traversing link $e \in E$

2.2. Concise Formulation of the bi-objective model for the ITFSDP

To illustrate the model framework, the concise formulation is presented in the following equations:

$$\min \sum_{w \in W} \sum_{r \in R_{\text{BSUE}}^w} \pi_r^w G^w p_r^w + \alpha^{\text{weight}} \sum_{l \in L_{\text{fre}}} C_l^{\text{op}} f_l , \tag{1}$$

Subject to

$$H_l^{\min} \le h_l \le H_l^{\max}, \forall l \in L_{\text{fre}} , \tag{2}$$

$$h_l f_l = 1, \forall l \in L_{\text{fre}} , \tag{3}$$

$$\tau_{l,i,q}^{\text{dep}} = \tau_{l,i,q}^{\text{arr}} + \tau_{l,i,q}^{\text{dwell}}, \forall l \in L_{\text{sch}}, i \in S_l \setminus \{s_l^{M_l}\}, q = 1,2,..,Q_l , \tag{4}$$

$$\tau_{\ell(e),t(e),q}^{\text{dep}} + T_e = \tau_{\ell(e),h(e),q}^{\text{arr}}, \forall e \in E, \ell(e) \in L_{\text{sch}}, q = 1,2,...,Q_{\ell(e)} , \tag{5}$$

$$\tau_{l,i,q}^{\text{dep}} \ge 0, \forall l \in L_{\text{sch}}, i \in S_l, q = 1,2,...,Q_l , \tag{6}$$

$$\tau_{l,s_l^1,1}^{\text{dep}} \le H_l^{\max}, \forall l \in L_{\text{sch}} , \tag{7}$$

$$H_l^{\min} \le \tau_{l,i,q+1}^{\text{dep}} - \tau_{l,i,q}^{\text{dep}} \le H_l^{\max}, \forall l \in L_{\text{sch}}, i \in S_l \setminus \{s_l^{M_l}\}, q = 1,2,...,Q_l - 1, \tag{8}$$

$$0 \le \tau_{l,i,q}^{\text{arr}} \le T, \forall l \in L_{\text{sch}}, i \in S_l, q = 1,2,...,Q_l , \tag{9}$$

$$\tau_{l,i,q}^{\text{dwell}} \ge D_{l,i}^{\min}, \forall l \in L_{\text{sch}}, i \in S_l \setminus \{s_l^{M_l}\}, q = 1,2,..,Q_l , \tag{10}$$

$$p_r^w = \frac{\exp\left(-\theta\left(\pi_r^w - \min\left(\pi_{r''}^w : r'' \in R_{\text{BSUE}}^w\right) - \eta\right)\right) - 1}{\sum_{r' \in R_{\text{BSUE}}^w} \exp\left(-\theta\left(\pi_{r'}^w - \min\left(\pi_{r''}^w : r'' \in R_{\text{BSUE}}^w\right) - \eta\right)\right) - 1}, \forall w \in W, r \in R_{\text{BSUE}}^w , \tag{11}$$

$$\sum_{r \in R_{\text{BSUE}}^w} p_r^w = 1 \; \forall w \in W \;\; , \tag{12}$$

$$p_r^w \ge 0, \forall w \in W, r \in R_{\text{BSUE}}^w . \tag{13}$$

Two objectives are considered, and we use the weighted sum method to aggregate them into one objective function. The first term in objective function (1) corresponds to the total passengers' generalised travel cost, in which π_r^w is the generalised travel cost of path $r \in R^w$, and $G^w p_r^w$ is the number of passengers travelling via the path. The second term in the objective function corresponds to the frequency-dependent operation cost, which is obtained by multiplying the total frequency by a frequency-dependent operation cost parameter (Fan and Machemehl 2006; Tirachini et al. 2010). The two costs are generally conflicting; a higher frequency corresponds to lower generalised passenger travel costs owing to the reduction in the passengers' waiting time but higher operation costs.

Equations (2) and (3) are the operational constraints for the frequency-based lines. Equation (2) ensures that the maximum and minimum headway values for the frequency-based lines are adhered to. Equation (3) defines the reciprocal relationship between the frequency and headway.

The operational constraints for the schedule-based services are presented as Equations (4)–(10). Equation (4) indicates that the departure time of the q^{th} run of line $l \in L_{sch}$ from stop $i \in S_l$ is determined by the vehicle's arrival and dwell times. Equation (5) indicates that the arrival time at the head node of link $e \in E$, $h(e)$, is the sum of the departure time from its tail node, $t(e)$, and travel time between the two consecutive stops via the line associated with the link, $\ell(e)$. Equation (6) is the nonnegativity constraint for departure times. According to Eq. (7), the first vehicle departs from the terminal before the maximum headway. Equation (8) represents the headway constraint for schedule-based lines. Equation (9) ensures that the last vehicle arrives at the last stop no later than the end of the modelling period. Equation (10) sets the minimum dwell time. Section 3.3.3 presents an equation for explicitly computing the dwell time.

Equations (11)–(13) represent the BSUE assignment constraints. Equation (11) specifies that between OD pair $w \in W$, the probability of selecting path $r \in R_{\text{BSUE}}^w$ depends on a scaling parameter θ as in the traditional SUE model (Sheffi 1985), bound parameter η, and generalised travel cost π_r^w. Equations (12) and (13) are definitional constraints. We formulate these constraints in a manner that is slightly different from that used in Watling et al. (2018). Our constraints are formulated explicitly using bounded choice set

R_{BSUE}^{w} that will be iteratively provided by the column-generation-and-reduction algorithm (see Section 3), while Watling et al. (2018)'s formulation is built upon all choices.

Because the proposed integrated model uses both frequencies and schedules as the decision variables, the optimal objective value obtained from the integrated optimisation model should be no greater than that of a model that optimises either frequency- or schedule-based lines. This is because the optimal solution to a model that optimises either the frequency or the schedule is a feasible solution to the integrated optimisation model, and a feasible solution cannot have a lower objective value than the optimal solution in a minimisation problem. This aspect stresses the significance of the proposed integrated optimisation approach. Moreover, this aspect implies that the objective value of the model that only optimises the frequency or schedule assigns an upper-bound value to the integrated model, inspiring us to develop a branch-and-bound algorithm.

2.3. Formulation of the Generalised Path Cost

The generalised path cost is defined as

$$\pi_r^w = \beta^{\text{inveh}} \sum_{e \in E_r^w} T_e + \beta^{\text{wait}} \sum_{i \in \mathcal{N}_r^{w,\text{transfer}} \cup \{o^w\}} t_{r,i}^{w,\text{wait}} + \beta^{\text{cap}} \sum_{e \in E_r^w} t_{r,e}^{w,\text{cap}}, \forall w \in W, r \in R^w \quad . \tag{14}$$

The first term on the right-hand side represents the in-vehicle travel time cost. The second term represents the waiting time cost, with $t_{r,i}^{w,\text{wait}}$ described in Section 2.3.1. The third term aggregates the perceived congestion cost of all links traversed by path *r*, with $t_{r,e}^{w,\text{cap}}$ described in Section 2.3.2.

2.3.1. Waiting time

At boarding stop *i*, the waiting time of the passengers travelling between OD pair *w* via path *r* is the difference between the passengers' arrival and departure time values at that stop, expressed as

$$t_{r,i}^{w,\text{wait}} = t_{r,i}^{w,\text{dep}} - t_{r,i}^{w,\text{arr}}, \forall w \in W, r \in R^w, i \in N_r^{w,\text{transfer}} \cup \{o^w\}, \tag{15}$$

where the passengers' arrival time $t_{r,i}^{w,\text{arr}}$ is defined as

$$t_{r,o^w}^{w,\text{arr}} = TD^w, \forall w \in W, r \in R^w \text{, and} \tag{16}$$

$$t_{r,h(e)}^{w,\mathrm{arr}} = t_{r,t(e)}^{w,\mathrm{dep}} + T_e \ , \forall w \in W, r \in R^w, e \in E_r^w \ . \tag{17}$$

Equation (16) indicates that the arrival time at the first stop (origin) equals the departure time of that OD pair. According to Equation (17), the arrival time at the head node of the link traversed by passengers is computed by adding the link travel time to the departure time at the tail node of the link.

Under the assumption that passengers board the first arriving vehicle, the following conditions hold if the line that users board at node i, $\ell\left(e_{r,i}^{w,\mathrm{board}}\right)$, is a schedule-based line.

$$t_{r,i}^{w,\mathrm{arr}} \le \tau_{l,i,1}^{\mathrm{dep}}, \text{ if } \Delta_{r,l,i,1}^{w,\mathrm{board}} = 1, \forall w \in W, r \in R^w, i \in N_r^{w,\mathrm{transfer}} \cup \left\{o^w\right\}, l = \ell\left(e_{r,i}^{w,\mathrm{board}}\right) \in L_{\mathrm{sch}} \ , \tag{18}$$

$$\tau_{l,i,q-1}^{\mathrm{dep}} < t_{r,i}^{w,\mathrm{arr}} \le \tau_{l,i,q}^{\mathrm{dep}}, \text{ if } \Delta_{r,l,i,q}^{w,\mathrm{board}} = 1, \forall w \in W, r \in R^w, i \in N_r^{w,\mathrm{transfer}} \cup \left\{o^w\right\}, l = \ell\left(e_{r,i}^{w,\mathrm{board}}\right) \in L_{\mathrm{sch}}, 1 < q \le Q_l \ , \tag{19}$$

$$\sum_{q=1}^{Q_l} \Delta_{r,l,i,q}^{w,\mathrm{board}} = 1, \forall w \in W, r \in R^w, i \in N_r^{w,\mathrm{transfer}} \cup \left\{o^w\right\}, l = \ell\left(e_{r,i}^{w,\mathrm{board}}\right) \in L_{\mathrm{sch}} \tag{20}$$

If passengers board the first run of a line, Equation (18) holds; otherwise, Equation (19) holds. Equation (20) specifies that users only board one vehicle at a stop. Passengers' departure time, $t_{r,i}^{w,\mathrm{dep}}$, depends on the line boarded and can be mathematically expressed as

$$t_{r,i}^{w,\mathrm{dep}} = t_{r,i}^{w,\mathrm{arr}} + \frac{1}{2} h_l + \tau_{l,i}^{\mathrm{dwell}}, \forall w \in W, r \in R^w, i \in N_r^{w,\mathrm{board}} \cup \left\{o^w\right\}, l = \ell\left(e_{r,i}^{w,\mathrm{board}}\right) \in L_{\mathrm{fre}} \ , \text{and} \tag{21}$$

$$t_{r,i}^{w,\mathrm{dep}} = \sum_{q=1}^{Q_l} \Delta_{r,l,i,q}^{w,\mathrm{board}} \tau_{l,i,q}^{\mathrm{dep}}, \forall w \in W, r \in R^w, i \in N_r^{w,\mathrm{board}} \cup \left\{o^w\right\}, l = \ell\left(e_{r,i}^{w,\mathrm{board}}\right) \in L_{\mathrm{sch}} \ . \tag{22}$$

According to Equation (21), if passengers board a frequency-based line, their departure time is the sum of their arrival time, expected waiting time approximated by half of the line's headway and dwell time. According to Equation (22), if passengers board a schedule-based line, they depart at the departure time of the vehicle that they board. Computation of the dwell time, $\tau_{l,i}^{\mathrm{dwell}}$, is described in Section 2.3.4.

2.3.2. Perceived congestion level associated with the capacity constraint

The perceived congestion levels for seated and non-seated passengers are distinguished and formulated as

$$\begin{cases} t_e^{\mathrm{cap,seat}} = \alpha_0 + \alpha_1 v_e^{\mathrm{onboard}}, \text{ if } v_e^{\mathrm{onboard}} \le Cap_{\ell(e)}^{\mathrm{seat}}; \\ t_e^{\mathrm{cap,stand}} = \alpha_0 + \alpha_1 v_e^{\mathrm{onboard}} + \alpha_2 \left(v_e^{\mathrm{onboard}} - Cap_{\ell(e)}^{\mathrm{seat}}\right) + \alpha_3 \Delta_e^{\mathrm{congest}}, \text{otherwise} \end{cases} , \forall e \in E \ , \tag{23}$$

where $\Delta_e^{\mathrm{congest}}$ indicates whether link e is congested and defined as

$$\Delta_e^{\text{congest}} \begin{cases} =1, \text{ if } v_e^{\text{onboard}} \le Cap_{\ell(e)}^{\text{seat}} \\ =0, \text{ if } v_e^{\text{onboard}} > Cap_{\ell(e)}^{\text{seat}} \end{cases}, \forall e \in E \ . \tag{24}$$

In Equation (23), if the number of onboard passengers is smaller than the capacity, implying that all passengers onboard may be seated, the seating capacity cost is a linear function of the number of onboard passengers. When the number of onboard passengers is larger than the capacity, two penalty terms are incorporated: one term based on the number of standing passengers, and the other term representing a constant penalty, capturing the stepwise increase in the congestion cost.

The perceived congestion level associated with link e on path r can be computed as

$$t_{r,e}^{w,\text{cap}} = \Delta_{r,e}^{w,\text{seat}} t_e^{\text{cap,seat}} + \left(1-\Delta_{r,e}^{w,\text{seat}}\right) t_e^{\text{cap,stand}}, \forall w \in W, r \in R^w, e \in E_r^w \ , \tag{25}$$

where $\Delta_{r,e}^{w,\text{seat}}$ is a binary variable indicating whether the passengers of OD pair w using path r have a seat when traversing link e, defined as

$$\Delta_{r,e}^{w,\text{seat}} \begin{cases} =1, \text{ if the passengers travelling via route } r \text{ have a seat} \\ =0, \text{ otherwise} \end{cases}, \forall w \in W, r \in R^w, e \in E_r^w . \tag{26}$$

Equation (25) implies that the congestion cost associated with the capacity constraint differentiates between sitting and standing. To identify passengers' seating status, the following constraints are devised.

$$\Delta_{r,e_l^k}^{w,\text{seat}} \le \Delta_{r,e_l^{k+1}}^{w,\text{seat}}, \forall w \in W, r \in R^w, l \in L, k = 1,2,...,\left|A_l\right|-1, \text{ and } e_l^k, e_l^{k+1} \in A_l \cap E_r^w \ , \tag{27}$$

$$\Delta_{r,e_l^k}^{w,\text{seat}} = \Delta_{e_l^k}^{\text{congest}}, \forall w \in W, r \in R^w, l \in L, k = 1,2,...,\left|A_l\right|, e_l^k \in A_l \cap E_r^w, t\left(e_l^k\right) \in N_r^{w,\text{transfer}} \cup \left\{o^w\right\} , \tag{28}$$

$$\Delta_{r,e_l^{k+1}}^{w,\text{seat}} \ge \Delta_{e_l^{k+1}}^{\text{congest}} \ , \forall w \in W, r \in R^w, l \in L, k = 1,2,...,\left|A_l\right|-1, \text{ and } e_l^k \in A_l \cap E_r^w \ , \tag{29}$$

$$\Delta_{e_l^{k+1}}^{\text{congest}} + \Delta_{r,e_l^k}^{w,\text{seat}} \ge \Delta_{r,e_l^{k+1}}^{w,\text{seat}} \ , \ \forall w \in W, r \in R^w, l \in L, k = 1,2,...,\left|A_l\right|-1, \text{ and } e_l^k \in A_l \cap E_r^w \ . \tag{30}$$

According to Equation (27), if passengers have a seat on the k^{th} link of line l, e_l^k, they remain seated on the subsequent link traversed by line l if they do not transfer to other lines. Eqs. (28)–(30) establish the link between the congestion status and seating status. Equation (28) indicates that at a boarding stop, the passengers' seating status is in accordance with the congestion status of the link to be boarded. Equations (29) and (30) indicate that when passengers travel continuously from the k^{th} link to the $(k+1)^{\text{th}}$ link of line

l, if link e_l^k is congested and link e_l^{k+1} is not, they have a seat on link e_l^{k+1}. The correctness of these equations is demonstrated in Appendix E.

To facilitate the formulation of v_e^{onboard} in Equation (23), we consider three consecutive intermediate stops traversed by line l, $\left(s_l^{k-1}, s_l^k, s_l^{k+1}\right), k = 2,..., M_l - 1$, and two links between the three nodes, e_l^{k-1} and e_l^k. The number of onboard passengers on link e_l^k is determined by the number of onboard passengers on the preceding link e_l^{k-1}, number of passengers alighting from line l at node s_l^k, $v_{l,s_k^l}^{\text{alight}}$, and number of passengers boarding line l at node s_k^l, $v_{l,s_k^l}^{\text{board}}$. Mathematically, this value can be expressed as

$$v_{l,s_l^1}^{\text{alight}} = 0, \forall l \in L, \tag{31}$$

$$v_{e_l^1}^{\text{onboard}} = v_{l,s_l^1}^{\text{board}}, \forall l \in L, \tag{32}$$

$$v_{e_l^k}^{\text{onboard}} = v_{e_l^{k-1}}^{\text{onboard}} - v_{l,s_l^k}^{\text{alight}} + v_{l,s_l^k}^{\text{board}}, \forall l \in L, k = 2,.., M_l - 1. \tag{33}$$

Equations (31) and (32) define the initial values for the alighting and onboard passengers. Equation (33) represents the formulation for the links between the second and last stops.

The abovementioned three equations are used only to illustrate the concept. For schedule-based services, we can trace the number of passengers boarding a particular run based on the schedule and passengers' arrival time. Thus, an additional subscript q is introduced for indexing a run in the equations. For frequency-based services, we cannot identify the bus or vehicle boarded by the passengers as no timetable information is available. Nevertheless, the passengers' boarding and alighting time values can be determined through variables $t_{r,s_l^k}^{w,\text{dep}}$ and $t_{r,s_l^k}^{w,\text{arr}}$, respectively. To use this information to compute the congestion cost, we divide the planning horizon into a set of time intervals. Passengers boarding the same frequency-based line in the same time interval are aggregated. A similar idea was adopted by Schmöcker et al. (2008). The detailed formulations are presented in Appendix B.

2.3.3. Dwell time

The dwell time for line l at stop i is computed as

$$\tau_{l,i}^{\text{dwell}} = \max\left(D_{l,i}^{\min}, \alpha_4 \max\left(v_{l,i}^{\text{alight}}, v_{l,i}^{\text{board}}\right)\right), \forall l \in L, i \in S_l \setminus \left\{s_l^{M_l}\right\}. \tag{34}$$

This term takes the higher value from the minimum dwell time of line *l* at stop *i*, $D_{l,i}^{\min}$, and the time required for passengers to board and alight. Intuitively, α_4 is interpreted as the average time for a passenger to board/alight a bus. Practically, this term can be obtained via a survey and specified for different types of vehicles and platforms to achieve high accuracy. Nevertheless, in this study, we assume a homogeneous value and use $\max\left(v_{l,i}^{\text{alight}}, v_{l,i}^{\text{board}}\right)$ to compute the critical number of passengers that determines the boarding and alighting time by implicitly assuming that passengers use different doors for boarding and alighting. This aspect is consistent with the bus operation in the Copenhagen metropolitan area, in which the front door of the bus is used for boarding, and the back door is used for alighting. If there is only one door and boarding is only allowed after alighting, $\max\left(v_{l,i}^{\text{alight}}, v_{l,i}^{\text{board}}\right)$ should be replaced with $\left(v_{l,i}^{\text{alight}} + v_{l,i}^{\text{board}}\right)$.

2.4. Solution Existence and Uniqueness

The existence of a solution to the proposed model (concise formulation in Section 2.2) depends on two conditions: 1) Whether there exists a feasible frequency and schedule setting that satisfies the operational constraints (Equations (2)–(10)); and 2) Given a feasible frequency and schedule setting, whether there exists a feasible BSUE flow solution. The feasibility of operational constraints (i.e., Equations (2)–(10)) can be evaluated in a straightforward manner. In the following analysis, we investigate the second condition.

Denoting $\mathcal{X} = \left\{\left(\mathbf{f}, \mathbf{h}, \boldsymbol{\tau}\right)\right\}$ as the set of frequency and timetable settings that satisfy the operational constraints, we present the following proposition.

Proposition 1: If $\mathcal{X} \neq \varnothing$ and $\eta \geq 0$, a feasible solution always exists when $\left|R_{\text{BSUE}}^{w}\right| = 1, \forall w \in W$.

Proof. $\mathcal{X} \neq \varnothing$ means that there exists a solution that satisfies the operational constraints. We only need to show that there exists a feasible BSUE flow distribution. As $\left|R_{\text{BSUE}}^{w}\right| = 1$, the difference between the maximum and minimum path costs is zero, which is less than or equal to a nonnegative η. In other words, by assigning all passengers to the only path in the choice set, constraints (11)–(13) can be satisfied. Therefore, a feasible solution to the problem exists.

This proposition indicates that if there is only one path in the choice set, there always exists a feasible BSUE solution despite the bounding value η. This property enables us to develop a column generation method starting with one path to solve the problem.

Proposition 2: Multiple solutions for the optimisation problem can exist.

Proof. This aspect is proved using the example in Appendix C.

According to the example in Appendix C, the existence of multiple optimal solutions can be attributed to the trade-off among different path attributes, i.e., waiting and congestion. Notably, this trade-off implies that even if the policymakers impose additional constraints on the transit operator for several cost components, i.e., maximum transfer waiting time or maximum congestion level, a global optimal design can be obtained by compromising other attributes. Moreover, this aspect demonstrates that the model formulation is flexible as the cost components between the frequency- and schedule-based lines can be reallocated, i.e., by reducing the waiting time cost for the frequency-based service but increasing the perceived congestion cost for the schedule-based services. This aspect justifies the benefits of the integrated design of frequency- and schedule-based services. It can easily be shown (Appendix D) that a feasible solution to the problem may not exist if the choice set is not properly determined. The example in Appendix D indicates that the infeasibility occurs because the input choice set violates the requirements of the BSUE constraints, rendering it risky to use a *k*-shortest path method to generate the initial choice set as the solution existence cannot be ensured.

3. SOLUTION METHOD

The proposed model is a mixed integer nonlinear programming (MINP) problem owing to Equations (1), (3), (11), (22) and (25), even though the logical constraints can be rewritten as linear constraints in a straightforward manner, including Equations (18), (19), (23), and (25). The basic concept underlying a typical algorithm for solving the MINP problem is to relax the problem to a nonlinear programming problem or MILP problem and generate and refine bounds by solving the relaxed problem (Bonami et al. 2012). Considering this concept, we use various techniques to obtain a relaxed MILP formulation and develop a branch-and-bound algorithm to solve it, given that the upper and lower bounds of the relaxed formulation can be derived. Because the problem formulation requires knowledge of the choice set, R^{w}_{BSUE}, as an input for the assignment constraints, we embed a column generation-and-reduction phase in the algorithm. In the following subsections, we present an overview of the solution algorithm, followed by an explanation of the key steps.

3.1. Overview of the Solution Algorithm

The process flow of the generic solution algorithm can be summarised as follows.

Step 1. Initialisation.

Step 1.1. Set iteration counter I as 0.

Step 1.2. Generate an initial feasible frequency and timetable setting, denoted as $\left[\mathbf{f}^{I}, \mathbf{h}^{I}, \boldsymbol{\tau}^{I}\right]$, where $\mathbf{f} = \left[f_l\right]$, $\mathbf{h} = \left[h_l\right]$, and $\boldsymbol{\tau}^{I} = \left[\tau^{\text{dep}}_{l,i,q}\right]$.

Step 1.3. Generate an initial path set $R^{w,I}$ for each OD pair $w \in W$ (Section 3.2).

Step 2. Solving the relaxed model.

Step 2.1. Formulate the relaxed integer linear problem by using the generated path set information (Section 3.3).

Step 2.2. Solve the relaxed problem by using the branch-and-bound method (Section 3.4).

If a solution is obtained, denote the solution as $\left[\mathbf{f}^{I+1}, \mathbf{h}^{I+1}, \boldsymbol{\tau}^{I+1}\right]$; otherwise, terminate the solution algorithm.

Step 3. Column generation-and-reduction.

Step 3.1. Generate a new path set $\bar{R}^{w,I}$ for each OD pair $w \in W$ (Section 3.2).

Step 3.2. Compare path sets $\bar{R}^{w,I}$ and $R^{w,I}$.

1) If $\bar{R}^{w,I} = R^{w,I}, \forall w \in W$, terminate the algorithm and output the optimal solution.

2) Denote the path cost associated with path r in path sets $\bar{R}^{w,I}$ and $R^{w,I}$ as $\tilde{\pi}^{w,I}_{r}$ and $\pi^{w,I}_{r}$, respectively.

a) Column generation.

If $\exists r \in \bar{R}^{w,I}$ and $r \notin R^{w,I}$ with $\tilde{\pi}^{w,I}_{r} \le \min\left\{\min_{r' \in \bar{R}^{w,I}} \tilde{\pi}^{w}_{r'}, \min_{r'' \in R^{w,I}} \pi^{w}_{r''}\right\} + \eta, \forall w$, update path set $R^{w,I+1} = R^{w,I} \cup \left\{r\right\}, \forall w$.

b) Column reduction.

If $\exists r \in R^{w,I+1}$ and $\tilde{\pi}^{w,I}_{r} > \min\left\{\min_{r' \in \bar{R}^{w,I}} \tilde{\pi}^{w}_{r'}, \min_{r'' \in R^{w,I}} \pi^{w}_{r''}\right\} + \eta, \forall w$, update path set $R^{w,I+1} = R^{w,I} \setminus \left\{r\right\}, \forall w$.

Set $I = I + 1$ and return to Step 2.

In Step 1, the existing frequency and timetable setting can be used as the initial feasible solution, and an initial path set can be generated using the label-setting algorithm developed by Florian (2004). Step 3 represents the column generation-and-reduction phase, in which the newly generated path set is compared with the existing path set. If a newly generated path satisfies the path set requirement of the BSUE, it is added to the existing path set. If an existing path violates the requirement, it is removed from the existing path set. If any perturbation occurs to the path set, a new relaxed formulation based on the updated path set is solved (return to Step 2); otherwise, the algorithm is terminated. The algorithm convergence depends on whether the new path set generated is different from the existing path set. In the worst case, when all of the paths in a network are included in the path set, the algorithm is terminated. Moreover, in Step 2.2, the algorithm terminates when there is no feasible solution to the relaxed MILP problem because of the large choice set, as illustrated in Appendix D.

3.2. Relaxed Formulation

The nonlinear expressions can be categorised as expressions with binary variables, if-then constraints, bilinear equations, and BSUE constraints. The following subsections introduce the linearisation techniques for only the BSUE and bilinear constraints as the BSUE constraints are developed for the first time in this study and the latter constraints are used in defining the ε-feasible solution algorithm.

3.2.1. BSUE constraints

Following the work of Liu and Wang (2015), to linearise the BSUE constraints, we first transform Equation (11) into equivalent constraints with logarithmic expressions and use a set of equations to linearise the logarithmic expressions. First, we reformulate Equation (11) considering the fraction between the probabilities of two paths r and r' as

$$\frac{p_r^w}{p_{r'}^w} = \frac{\exp\left(-\theta\left(\pi_r^w - \min\left\{\pi_{r''}^w : r'' \in R_{\text{BSUE}}^w\right\} - \eta\right)\right) - 1}{\exp\left(-\theta\left(\pi_{r'}^w - \min\left\{\pi_{r''}^w : r'' \in R_{\text{BSUE}}^w\right\} - \eta\right)\right) - 1}, \forall w \in W, r, r' \in R_{\text{BSUE}}^w, r \neq r'. \quad (35)$$

Subsequently, we introduce an auxiliary variable y_r^w, defined as

$$y_r^w = \exp\left(-\theta\left(\pi_r^w - \min\left\{\pi_{r''}^w : r'' \in R_{\text{BSUE}}^w\right\} - \eta\right)\right) - 1, \forall r \in R_{\text{BSUE}}^w, w \in W. \tag{36}$$

Next, Equation (35) is reformulated as

$$\ln\left(p_r^w\right) - \ln\left(p_{r'}^w\right) = \ln\left(y_r^w\right) - \ln\left(y_{r'}^w\right), \forall r, r' \in R_{\text{BSUE}}^w, r \neq r', w \in W. \tag{37}$$

By introducing two more auxiliary variables χ_r^w and z_r^w, we transform Equation (37) into the following equations:

$$\chi_r^w - \chi_{r'}^w = z_r^w - z_{r'}^w, \forall r, r' \in R_{\text{BSUE}}^w, r \neq r', w \in W, \tag{38}$$

$$\chi_r^w = \ln\left(p_r^w\right), \forall r \in R_{\text{BSUE}}^w, w \in W, \tag{39}$$

$$z_r^w = \ln\left(y_r^w\right), \forall r \in R_{\text{BSUE}}^w, w \in W. \tag{40}$$

In addition, we reformulate Eq. (36) as

$$\ln\left(y_r^w + 1\right) = -\theta\left(\pi_r^w - \min\left\{\pi_{r''}^w : r'' \in R_{\text{BSUE}}^w\right\} - \eta\right), \forall r \in R_{\text{BSUE}}^w, w \in W. \tag{41}$$

Through this formulation, we can apply the techniques developed by Liu and Wang (2015) to linearise the logarithmic expressions.

3.2.2. Bilinear equations

There are two bilinear terms in the model, objective function (1) and constraint (3). Following the work of Adjiman et al. (1998), bilinear terms are approximated by their convex envelope. For example, for constraint (3), given the ranges of headway, $\left[\underline{h}, \overline{h}\right]$, and frequency, $\left[\underline{f}, \overline{f}\right]$, the following equations approximate bilinear constraint (3):

$$1 \geq \underline{h}_l f_l + h_l \underline{f}_l - \underline{h}_l \underline{f}_l, \forall l \in L_{\text{fre}}, \tag{42}$$

$$1 \geq \overline{h}_l f_l + h_l \overline{f}_l - \overline{h}_l \overline{f}_l, \forall l \in L_{\text{fre}}, \tag{43}$$

$$1 \leq \overline{h}_l f_l + h_l \underline{f}_l - \overline{h}_l \underline{f}_l, \forall l \in L_{\text{fre}}, \tag{44}$$

$$1 \leq \underline{h}_l f_l + h_l \overline{f}_l - \underline{h}_l \overline{f}_l, \forall l \in L_{\text{fre}}. \tag{45}$$

The relaxation of the bilinear constraints may lead to infeasible solutions to the problem because the solution to the relaxed formulation can only be guaranteed to satisfy constraints (42)–(45) instead of the original reciprocal constraint (3). To address this issue, we define the ε-feasibility, which can be mathematically expressed as follows:

Definition: $(\mathbf{f},\mathbf{h})$ is ε-feasible if it satisfies constraints (2), (4)–(13), (42)–(45), and

$$\left|h_l f_l - 1\right| \le \varepsilon, \forall l \in L_{\text{fre}} \ . \tag{46}$$

Accordingly, we can define an optimal ε-feasible solution as the optimal solution that satisfies constraint (46) instead of constraint (3).

3.3. Branch-and-Bound Method

To solve the relaxed formulation in Step 2 of the algorithm described in Section 3.1, a branch-and-bound algorithm is developed. In the algorithm, the frequencies of the frequency-based transit lines are the branching variables. Each node in the branch-and-bound tree is associated with a feasible frequency region, and new branches are generated by evenly dividing the feasible region into two. The lower bound value associated with each node is obtained by solving the relaxed MILP problem formulated using the techniques introduced in Section 3.2, whereas the upper-bound value is obtained by solving the relaxed MILP problem based on a fixed frequency.

4. NUMERICAL EXAMPLES

Experiments are conducted to illustrate the properties of the formulation and performance of the solution algorithm. The input data for the experiments are available in a GitHub repository (https://github.com/hkujy/NDPwithBSUE).

4.1. Schedule-Synchronisation ‘Paradox’

In this test, we demonstrate a novel paradoxical phenomenon under the BSUE. A two-link network is constructed, as shown in Figure 1. The network contains two schedule-based lines, with each line containing one vehicle to be scheduled. The seating capacity of the two lines is 50 and 100, respectively. The generalised travel cost function associated with each link is marked next to the link. A before-and-after study is conducted. In the before and after scenarios, the scheduled departure of line 2 pertains to time 10 and 0, respectively.

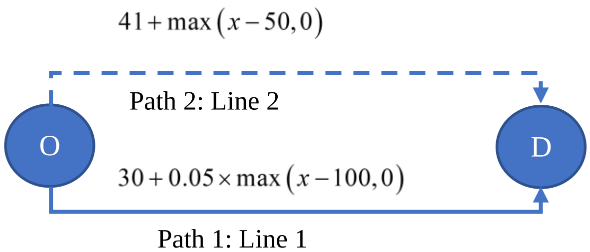

Demand = 150; departure time is 0; $\eta = 10$; $\theta = 0.15$.

	Departure time	
	Before	After
Line 1	0	0
Line 2	10	0

* Note: x in the function represents the number of passengers travelling via the link

Figure 1 Network and data for demonstrating the paradoxical phenomenon

The results of the two scenarios are presented in Table 2. The last column shows that the total generalised travel cost for the passengers is larger in the after scenario. This finding highlights a paradoxical phenomenon that well-synchronised transit services can deteriorate the network performance measured by the total generalised travel cost of the passengers. Similar to Braess' paradox (Sheffi 1985; Nagurney and Boyce 2005; Braess et al. 2005), the occurrence of the paradox is rooted in the passengers' perception error and the consideration of congestion cost on a crowded bus.

Table 2 Results of the before-and-after study for demonstrating the paradoxical phenomenon

Cases	Paths	Whether a path is used	Path flow	Generalised path travel cost	Total generalised travel cost
Before	Path 1	Yes	150.00	32.50	4875.00
	Path 2	No	-	(51.00)	
After	Path 1	Yes	142.48	32.12	4885.34
	Path 2	Yes	7.52	41.00	

Compared with the well-known Braess' paradox, the originality of our results is twofold. First, we consider the SUE with a bounded choice model, and thus, this study represents the first attempt at investigating the paradoxical phenomenon under such a travel behaviour assumption. Second, we consider the schedule synchronisation in the transit network, which is a different scenario than that considered in Braess' example, implying that it may not always be beneficial to create a synchronised timetable to reduce the total generalised travel cost of the passengers.

4.2. Effect of η on the Solution

Watling et al. (2018) proved that when η approaches infinity, the MNL SUE model becomes a special case of the BSUE model. However, the operator must understand the influence of different behaviour assumptions on the network design solutions and the effect of changes in η on the scheduling results. This aspect is illustrated in this experiment. Consider a network with two nodes and three parallel schedule-based lines connecting the two nodes. The link travel times associated with the three lines are 15, 18, and 23 min, respectively. We consider 100 passengers departing from origin A at time 5 towards destination B. Because this experiment is aimed at examining the solutions at different η values, we mitigate the congestion effects by setting the seating capacity of each bus line as 100 and the congestion coefficients in Equation (23) as $\alpha_0 = 0, \alpha_1 = 0.01, \alpha_2 = 0$, and $\alpha_3 = 0$.

Tables 3(a)–(b) list the timetable, path cost, and total generalised travel cost obtained under different η values and those defined using the SUE model, respectively. When the BSUE model is used, the departure time of line 1 is set as 5, which synchronises with the passengers' departure time. The corresponding values for the other two lines are zero, implying that they are not used by the passengers departing at time 5, resulting in zero flow. This phenomenon occurs because the BSUE allows the path choice probability to be 0 or 1, thereby avoiding the assignment of flow to long paths. Therefore, the optimal timetable is set in a manner that ensures that passengers use only one path, i.e., the path with the least travel time. In contrast, under the SUE, the departure times of all three lines are synchronised with the passengers' departure times.

This example demonstrates that the travel behaviour model affects the network design solution. The effects can be attributed to the assumption of the passenger choice set, which determines the setting of the timetable to synchronise with the passengers' departure times to minimise their total generalised travel cost. In general, the total generalised travel cost based on the BSUE is expected to be lower than that based on the SUE as the BSUE limits the size of detours that a passenger is willing to make, and the probabilities below the bounds are adjusted proportionally. If the network is optimised based on one of the two conditions, the optimised networks will be different when the BSUE or SUE are used; however, the BSUE-optimised network is unlikely to have a higher cost than the SUE-optimised network.

Table 3 Effect of η on the solution

(a) Departure time results

	$\eta=1$	$\eta=3$	$\eta=5$	SUE
Line 1	5	5	5	5
Line 2	0	0	0	5
Line 3	0	0	0	5

(b) Path cost and probability

	$\eta=1$		$\eta=3$		$\eta=5$		SUE	
	π_p^w	p_r^w	π_r^w	p_r^w	π_r^w	p_r^w	π_r^w	p_r^w
Path 1 via Line 1	16	1.00	16	1.00	16	1.00	15.5	0.51
Path 2 via Line 2	18	0.00	18	0.00	18	0.00	18.3	0.33
Path 3 via Line 3	23	0.00	23	0.00	23	0.00	23.2	0.16
Total generalised travel cost	1600		1600		1600		1767.5	

4.3. Seating Constraints and Dwell Time

The four-node network in Figure 2 is considered to highlight the merits and demerits of the seating capacity constraints. The network contains two lines: both lines are set to be schedule-based, and each line has one vehicle to be scheduled with 100 seats. Three OD relations are considered: 60, 60, and 10 passengers travelling from nodes A to D, A to B, and B to D, respectively. All passengers depart at time 0.

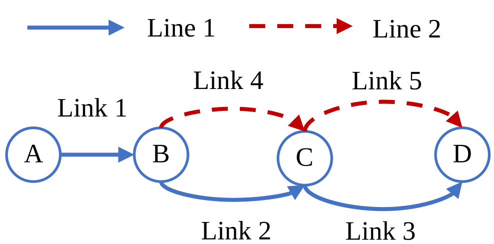

Link No.	Transit line	Tail Node	Head node	Travel time
1	1	A	B	5
2	1	B	C	4
3	1	C	D	3
4	2	B	C	2
5	2	C	D	4

Figure 2 Four-node network

Figure 3 plots the trajectories of bus line 1 and one passenger path between OD pair AD. Figure 3 (a) also indicates the minimum dwell time and additional dwell time associated with boarding and alighting. In Figure 3 (b), the values of $\Delta_{r,e}^{\text{seat}}$ are marked next to the trajectory with different colours. $\Delta_{r,1}^{\text{seat}}=0$ because 120 passengers from OD pairs AB and AD board at stop A, rendering the vehicle congested, with several passengers left without a seat. At stop B, passengers of OD pair AB alight, the vehicle becomes uncongested, and passengers of OD pair AD take a seat. In this case, $\Delta_{r,4}^{\text{seat}} = \Delta_{r,5}^{\text{seat}} = 1$. This figure illustrates that the proposed seating capacity exhibits the following features: 1) When a passenger travels from a congested link to an uncongested link, the user can obtain a seat, and 2) once a passenger occupies a seat, the user remains seated if the user does not transfer to other lines. In addition, it is also demonstrated in Appendix F that differentiating the sitting and standing effect will affect the schedule and users' travel experience.

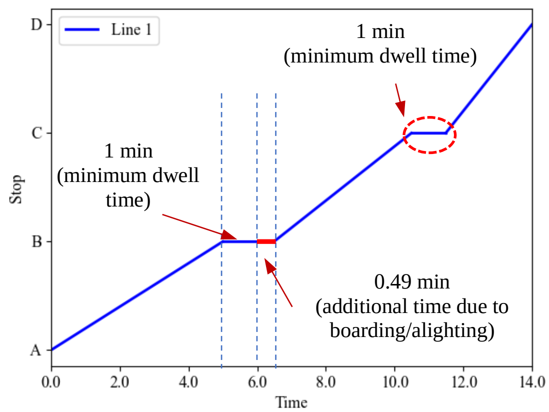

a) Trajectories of bus line 1

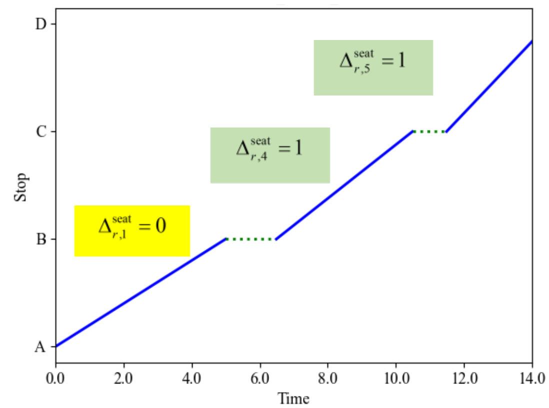

b) Trajectory of path (A → Link 1→Link 4 →Link 5 → D) between OD pair AD

Figure 3 Illustration of dwell time and seating constraints

A demerit of the method is that the seating status depends only on the aggregated congestion status. When passengers from various OD pairs mingle at one congested station, a more accurate estimation must be performed to determine the number of standing and seating passengers for each path. However, in this case, it may be necessary to introduce additional nonlinear expressions to split the aggregated congestion flow among all paths based on a certain proportion, thereby increasing the model complexity. A similar issue is encountered when accounting for the boarding and alighting times in computing the passengers' path time. The boarding and alighting time values depend only on the aggregated passenger flow. When calculating the passengers' path time, it is possible that some passengers alight before others and have a lower value of alighting time. The alighting times cannot be differentiated by the current method. We leave this for future research.

4.4. Case Studies Based on the DTU–CPH Network

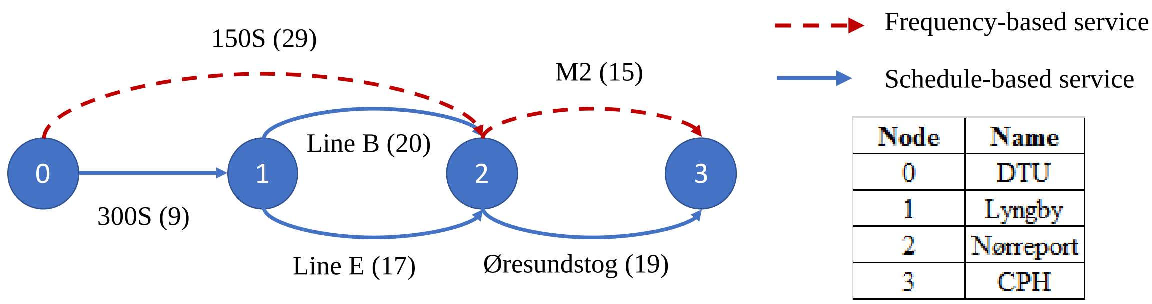

Node	Name
0	DTU
1	Lyngby
2	Nørreport
3	CPH

Figure 4 Main public transport services between DTU and CPH

The following numerical examples are based on the main public transport services between the Technical University of Denmark (DTU) and Copenhagen Airport (CPH), as shown in Figure 4. The travel times are marked in the parentheses next to the name of the line. We consider one hour of travel demand containing 20 passenger groups, in which every 3 min, a group of 10 passengers wishes to depart. The modelling horizon T is set to be 120 min to ensure that the last group of passengers arrive at their destination within the modelling period. The parameters are set as follows: $f_{\min} = 0.05$, $f_{\max} = 0.2$, $\beta^{\text{inveh}} = 0.43$, $\beta^{\text{wait}} = 0.575$, and $\theta = 0.15$. The algorithm is coded in C#, and the relaxation model is solved using CPLEX 12.7. The maximum computation time for the CPLEX solver and gap value are set as 2 h and 0.01, respectively. The program is implemented on a computer with an Intel® Xeon® CPU E5-2697 @ 2.30 GHz and 12 GB RAM processor.

4.4.1. Performance of the algorithm

According to our preliminary tests, if excessively many paths are included in the branch-and-bound algorithm, CPLEX cannot find a solution. Therefore, we add a restriction that only one new path can be added to the path set per iteration in the experiments and develop a path-adding strategy. The strategy computes a gap value for each newly generated path, which is the difference between its generalised travel cost and the minimum generalised cost connecting the same OD pair in the existing path set. The path that has the minimum gap value is selected to add to the existing path set.

Figure 5 shows the convergence of the algorithm for different values of η. The total generalised travel cost is not always decreased. This phenomenon can be attributed to three reasons. The first reason pertains to the paradoxical phenomenon described in Section 4.1. The second reason is that the column generated in each iteration in this study is the unused path that satisfies the bound choice set condition. This does not necessarily ensure that the objective is achieved, as the column generation method has been devised for solving large linear programming problems. Third, there exists a trade-off among different cost components when more paths are considered in the bounded choice set. Although a large path set can disperse the congestion cost and boarding and alighting time values, the path set could contain paths that have a higher in-vehicle travel time, thereby inducing a higher total generalised travel cost. The computation time values for $\eta = 1$, $\eta = 2$, and $\eta = 3$ are 115 min, 47 min, and 81 min, respectively. This shows that there may not exist a linear relationship between the computation time and η. In general, the computation time does not impede the application because the proposed model is used for planning (the operators in Copenhagen revise schedule/frequency every half year) and the operator can select a small set of lines to be optimised (such as the setting in this example). Nevertheless, the development of an efficient solution algorithm is essential for the application of this method in large networks.

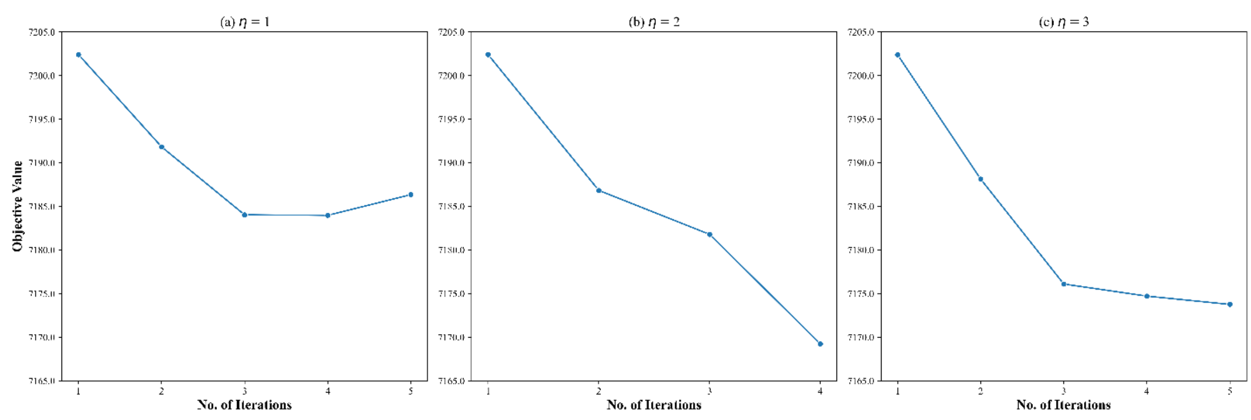

Figure 5 Objective values over iterations for different values of η

Notably, the value of η is used to characterise the user behaviour and must be calibrated from empirical studies. Decision makers should not arbitrarily set the value as 2, as in this example, to design the service based on the lower total generalised travel cost. Moreover, decision makers must implement the solution obtained in the last iteration and not the iteration pertaining to the minimum cost. For example, when $\eta = 1$, if the solution with the minimum objective is selected, several paths considered by the passengers may be overlooked by the decision makers, and the transit lines serving these paths may not be well coordinated. Therefore, when users travel these paths, they might encounter a higher generalised travel cost. In conclusion, the consideration of more realistic travel behaviour introduces not only additional complexity into the mathematical modelling but also difficulties associated with the interpretation of the results, as the results are not as straightforward as those obtained using models in which passengers are assumed to only travel via the shortest path or frameworks that do not contain a transit assignment model.

4.4.2. Trade-off between the operation cost and total generalised travel cost

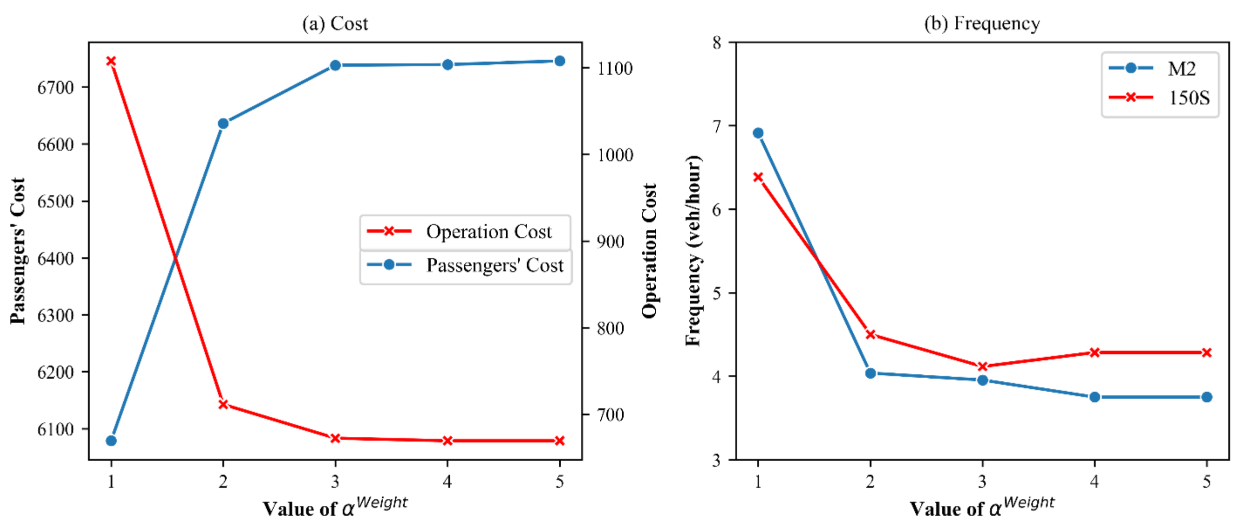

Figure 6 Effect of α^{weight}

To illustrate the trade-off between the operation cost and total travel cost, we set C^{op} as 5000 and increase the weighting parameter α^{weight} (which indicates the importance of the operation cost) from 1 to 5. The resultant operation and generalised travel costs are plotted in Figure 6 (a). A trade-off can be observed between the operation and generalised travel costs, which indicates that the reduction in the operation cost is accompanied by an increase in the passengers' generalised travel cost. Figure 6 (b) shows that the frequencies of the two frequency-based lines vary with the increase in α^{weight}.

5. CONCLUSION

A mixed integer nonlinear programming model was developed to optimise transit systems that consist of both frequency- and schedule-based services. The model can simultaneously determine the optimal frequencies for the frequency-based services and timetables for the schedule-based services while considering that the passengers' route choice behaviour follows the SUE with a bounded choice model. A set of constraints was established to model the passengers' seating behaviour, considering that a passenger who occupies a seat will remain seated at the subsequent stops of the same line. To solve the model, various linearisation techniques were used to reformulate the nonlinear model into a MILP model, which was then solved using a branch-and-bound algorithm. Numerical studies were conducted to demonstrate the properties of the formulation and performance of the solution method. The notable findings are summarised as follows: 1) We illustrated the occurrence of a novel schedule-synchronisation paradoxical phenomenon under the SUE with a bounded choice model. According to the 'paradox', a well-synchronised schedule can worsen the network performance indicated by the total generalised travel cost; 2) We compared the effects of different travel behaviour assumptions, i.e., BSUE and SUE, on the solution, and the results indicated that the design based on the BSUE could achieve a lower total generalised travel cost than that associated with the SUE.

This study can be extended in various directions. In particular, this study represents the first attempt at incorporating the state-of-the-art BSUE travel behaviour model for determining the transit frequency and schedule. This behavioural model can be incorporated into other transport network design problems. In addition, the BSUE implicitly assumes that passengers select the route set themselves. Future research can examine the scenario in which passengers make the decision based on the travel strategy (Marcotte et al. 2004; Zimmermann et al. 2021) or receive routing recommendations (Corman 2020; Jiang and Ceder 2021). Moreover, to obtain a model that can be implemented in practice and assist decision makers, it is desirable to develop a heuristic or metaheuristic solution method for large-network applications.

REFERENCES

Adjiman CS, Androulakis IP, Floudas CA (1998) A global optimisation method, αBB, for general twice-differentiable constrained NLPs-II. Implementation and computational results. *Comput. Chem. Eng.* 22:1159-1179.

Anderson MK, Nielsen OA, Prato CG (2017) Multimodal route choice models of public transport passengers in the Greater Copenhagen Area. *EURO J. Transp. Logist.* 6(3):221-245.

Ávila-Torres P, López-Irarragorri F, Caballero R, Ríos-Solís Y (2018) The multimodal and multiperiod urban transportation integrated timetable construction problem with demand uncertainty. *J. Ind. Manag. Optim.*14(2):447.

Bertsimas D, Ng YS, Yan J (2021). Data-Driven Transit Network Design at Scale. *Oper. Res.* 69(4):1118-1133.

Bertsimas D, Sian Ng Y, Yan J (2020) Joint frequency-setting and pricing optimization on multimodal transit networks at scale. *Transp. Sci.* 54(3):839-853.

Bonami P, Kilinç M, Linderoth J (2012) Algorithms and software for convex mixed integer nonlinear programs. *Mixed integer nonlinear programming* (Springer, New York), 1-39.

Borndörfer R, Grötschel M, Pfetsch ME (2007) A column-generation approach to line planning in public transport. *Transport. Sci.*41(1):123-132.

Braess D, Nagurney A, Wakolbinger T (2005) On a paradox of traffic planning. *Transport. Sci*. 39(4): 446-450.

Cancela H, Mauttone A, Urquhart ME (2015) Mathematical programming formulations for transit network design. *Transport. Res. B-Meth.* 77:17-37.

Cats O, West J, Eliasson J (2016) A dynamic stochastic model for evaluating congestion and crowding effects in transit systems. *Transport. Res. B-Meth.* 89:43-57.

Ceder A, Golany B, Tal O (2001) Creating bus timetables with maximal synchronisation. *Transport*. *Res. A-Pol*. 35:913–928.

Ceder A, Tal O (2001) Designing synchronisation into bus timetables. *Transp. Res. Record.* 1760: 28–33.

Ceder A, Wilson NH (1986) Bus network design. *Transport. Res. B-Meth.* 20(4): 331-344.

Chen Z, Li X, Zhou X (2019) Operational design for shuttle systems with modular vehicles under oversaturated traffic: Discrete modeling method. *Transport. Res. B-Meth.* 122:1-19.

Constantin I, Florian M (1995) Optimising frequencies in a transit network: a nonlinear bi-level programming approach. *Int. T. Oper. Res.* 2(2):149-164.

Corman, F (2020). Interactions and equilibrium between rescheduling train traffic and routing passengers in microscopic delay management: A game theoretical study. *Transport. Sci.* 54(3):785-822

Cortés CE, Jara-Moroni P, Moreno E, Pineda C (2013) Stochastic transit equilibrium. *Transport. Res. B-Meth.* 51:29-44.

De Cea J, Fernández E (1993) Transit assignment for congested public transport systems: an equilibrium model. *Transport. Sci.* 27(2):133-147.

Dell'Olio L, Ibeas A, Cecin P (2011) The quality of service desired by public transport users. *Transp. Policy*. 18(1):217-227.

Eltved M, Nielsen OA, Rasmussen TK (2019) An assignment model for public transport networks with both schedule-and frequency-based services. *EURO J. Transp. Logist.* 8(5):769-793.

Fan W, Machemehl RB (2006) Optimal transit route network design problem with variable transit demand: genetic algorithm approach. *J. Transp. Eng.* 132(1): 40-51.

Farahani RZ, Miandoabchi E, Szeto WY, Rashidi H (2013) A review of urban transportation network design problems. *Eur. J. Oper. Res.* 229(2): 281–302.

Florian M (2004) Finding shortest time-dependent paths in schedule-based transit networks: a label setting algorithm. *Schedule-based Dynamic Transit Modeling: Theory and Applications* (Springer US), 43-52.

Fouilhoux P, Ibarra-Rojas OJ, Kedad-Sidhoum S, Rios-Solis YA (2016) Valid inequalities for the synchronisation bus timetabling problem. *Eur. J. Oper. Res.* 251(2):442-450.

Gardner CB, Nielsen SD, Eltved M, Rasmussen TK, Nielsen OA, Nielsen BF (2021) Calculating conditional passenger travel time distributions in mixed schedule-and frequency-based public transport networks using Markov chains. *Transport. Res. B-Meth.*152:1-17.

Goerigk M, Schmidt M (2017) Line planning with user-optimal route choice. *Eur. J. Oper. Res.* 259(2):424-436.

Guihaire V, Hao JK (2008) Transit network design and scheduling: A global review. *Transport. Res. A-Pol.* 42(10):1251–1273.

Guo X, Sun H, Wu J, Jin J, Zhou J, Gao Z (2017). Multiperiod-based timetable optimisation for metro transit networks. *Transport. Res. B-Meth*. 96:46-67.

Hamdouch Y, Ho HW, Sumalee A, Wang G (2011) Schedule-based transit assignment model with vehicle capacity and seat availability. *Transport. Res. B-Meth.* 45(10):1805-1830.

Hussain E, Bhaskar A, Chung E (2021) Transit OD matrix estimation using smartcard data: Recent developments and future research challenges. *Transport. Res C-Emer.* 125: 103044.

Ibarra-Rojas OJ, Delgado F, Giesen R, Muñoz JC (2015) Planning, operation, and control of bus transport systems: A literature review. *Transport. Res. B-Meth.* 77:38-75.

Ibarra-Rojas OJ, López-Irarragorri F, Rios-Solis YA (2016) Multiperiod bus timetabling. *Transport. Sci.* 50(3):805-822.

Ibarra-Rojas OJ, Rios-Solis YA (2012) Synchronisation of bus timetabling. *Transport. Res. B-Meth.* 46(5):599-614.

Lee K, Jiang Y, Ceder A, Dauwels J, Su R, Nielsen OA (2022). Path-oriented synchronized transit scheduling using time-dependent data. *Transp. Res. Part C-Emerg. Technol.* 136:103505.

Leurent F, Chandakas E, Poulhès A (2014) A traffic assignment model for passenger transit on a capacitated network: Bi-layer framework, line sub-models and large-scale application. *Transport. Res. C-Emer*. 47:3-27.

Li ZC, Lam WH, Wong SC, Sumalee A (2010) An activity-based approach for scheduling multimodal transit services. *Transport.* 37(5):751-774.

Liu H, Wang DZ (2015) Global optimisation method for network design problem with stochastic user equilibrium. *Transport. Res. B-Meth.* 72:20-39.

Marcotte P, Nguyen S, Schoeb A (2004) A strategic flow model of traffic assignment in static capacitated networks. Oper. Res. 52(2): 191-212.

Martínez H, Mauttone A, Urquhart ME (2014) Frequency optimisation in public transportation systems: Formulation and metaheuristic approach. *Eur. J. Oper. Res.* 236(1):27-36.

Mesa JA, Ortega FA, Pozo MA (2014) Locating optimal timetables and vehicle schedules in a transit line. *Ann. Oper. Res.* 222(1): 439-455.

Movia, 2020a. https://www.moviatrafik.dk/media/6310/nyt-bynet-linje-150s.pdf. Retrieved 3rd Feb 2020.

Movia, 2020b. https://www.moviatrafik.dk/media/7455/udbudsmateriale-a18-engelsk-versiondocx.pdf. Retrieved 3rd Feb 2020.

Nagurney A, Boyce D (2005) Preface to "on a paradox of traffic planning". *Transport. Sci.* 39(4): 443-445.

Nielsen OA., Eltved M, Anderson MK, Prato CG (2021) Relevance of detailed transfer attributes in large-scale multimodal route choice models for metropolitan public transport passengers. *Transp. Res. Part A Policy Pract*., 147:76-92.

Nuzzolo A, Russo F, Crisalli U (2001) A Doubly Dynamic Schedule-based Assignment Model for Transit Networks. *Transport. Sci*. 35(3):268.

Schmidt M, Schöbel A (2015) Timetabling with passenger routing. *OR spectrum*. 37(1):75-97.

Schmöcker JD, Bell MG, Kurauchi F (2008) A quasi-dynamic capacity constrained frequency-based transit assignment model. *Transport. Res. B-Meth.* 42(10):925-945.

Schmöcker JD, Fonzone A, Shimamoto H, Kurauchi F, Bell MG (2011) Frequency-based transit assignment considering seat capacities. *Transport. Res. B-Meth.* 45(2):392-408.

Schöbel A (2017) An eigenmodel for iterative line planning, timetabling and vehicle scheduling in public transportation. *Transport. Res. C-Emer.* 74:348-365.

Shafiei S, Saberi M, Vu HL (2020) Integration of departure time choice modeling and dynamic origin–destination demand estimation in a large-scale network. *Transp. Res. Rec.* 2674(9), 972-981.

Sheffi Y (1985) *Urban transportation networks* (Prentice-Hall, Englewood Cliffs, NJ)

Szeto WY, Jiang Y (2014) Transit route and frequency design: Bi-level modeling and hybrid artificial bee colony algorithm approach. *Transport. Res. B-Meth.* 67:235-263.

Tang Y, Jiang Y, Yang H, Nielsen OA (2020) Modeling and optimizing a fare incentive strategy to manage queuing and crowding in mass transit systems. *Transport. Res. B-Meth.*138:247-267.

Tirachini A, Hensher DA, Jara-Díaz SR (2010) Comparing operator and users costs of light rail, heavy rail and bus rapid transit over a radial public transport network. *Res. Transp. Econ.* 29 (1):231-242.

Tirachini A, Hurtubia R, Dekker T, Daziano, RA (2017). Estimation of crowding discomfort in public transport: Results from Santiago de Chile. *Transp. Res. A.* 103:311-326.

Tirachini A, Sun L, Erath A, Chakirov A (2016). Valuation of sitting and standing in metro trains using revealed preferences. *Transport Policy* 47: 94-104.

Toledo T, Cats O, Burghout W, Koutsopoulos HN (2010) Mesoscopic simulation for transit operations. *Transp. Res. Part C-Emerg. Technol.* 18(6):896-908.

Wardman M, Whelan G (2011). Twenty years of rail crowding valuation studies: evidence and lessons from British experience. *Transp. Rev.* 31(3):379-398.

Watling DP, Rasmussen TK, Prato CG, Nielsen OA (2018) Stochastic user equilibrium with a bounded choice model. *Transport. Res. B-Meth.* 114:254-280.

Wong RCW, Yuen TWY, Fung KW, Leung JMY (2008) Optimising timetable synchronisation for rail mass transit. *Transport. Sci.* 42(1):57–69.

Yin J, D'Ariano A, Wang Y, Yang L, Tang T (2021) Timetable coordination in a rail transit network with time-dependent passenger demand. *Eur. J. Oper. Res.* 295(1):183-202.

Zhang C, Gao Y, Yang L, Gao Z, Qi J (2020) Joint optimisation of train scheduling and maintenance planning in a railway network: A heuristic algorithm using Lagrangian relaxation. *Transport. Res. B-Meth.* 134:64-92.

Zimmermann M, Frejinger E, Marcotte P (2021) A strategic markovian traffic equilibrium model for capacitated networks. *Transp. Sci*. 55(3): 574-591.